

BrainStack: Neuro-MoE with Functionally Guided Expert Routing for EEG-Based Language Decoding

Ziyi Zhao¹, Jinzhao Zhou¹, Xiaowei Jiang¹, Beining Cao¹, Wenhao Ma¹, Yang Shen¹, Ren Li², Yu-kai Wang¹, and Chin-Teng Lin^{1,*}

¹University of Technology Sydney, Sydney, Australia

²Mohamed bin Zayed University of Artificial Intelligence, Masdar City, UAE

ziyi.zhao-2@student.uts.edu.au, chin-teng.lin@uts.edu.au

Abstract

Decoding linguistic information from electroencephalography (EEG) remains challenging due to the brain’s distributed and nonlinear organization. We present BrainStack, a functionally guided neuro-mixture-of-experts (Neuro-MoE) framework that models the brain’s modular functional architecture through anatomically partitioned expert networks. Each functional region is represented by a specialized expert that learns localized neural dynamics, while a transformer-based global expert captures cross-regional dependencies. A learnable routing gate adaptively aggregates these heterogeneous experts, enabling context-dependent expert coordination and selective fusion. To promote coherent representation across the hierarchy, we introduce cross-regional distillation, where the global expert provides top-down regularization to the regional experts. We further release SilentSpeech-EEG (SS-EEG), a large-scale benchmark comprising over 120 hours of EEG recordings from 12 subjects performing 24 silent words—the largest dataset of its kind. Experiments demonstrate that BrainStack consistently outperforms state-of-the-art models, achieving superior accuracy and generalization across subjects. Our results establish BrainStack as a functionally modular, neuro-inspired MoE paradigm that unifies neuroscientific priors with adaptive expert routing, paving the way for scalable and interpretable brain-language decoding.

1. Introduction

The human brain is a highly organized and distributed system composed of approximately 86 billion neurons. These neurons interact through complex electrical activity, and their collective dynamics give rise to macroscopic field potentials known as brainwave signals. Electroencephalography (EEG) provides a non-invasive and high-temporal-

resolution technique for capturing large-scale cortical dynamics, making it particularly well-suited for real-time neural decoding [19]. With millisecond-level precision, modern EEG acquisition systems enable scalable and practical recording of neural signals across distributed brain regions [34]. These capabilities form the foundation for brain-computer interface (BCI) applications, especially in cognitive and communication tasks where timely and accurate decoding of brain activity is essential [31].

Despite its potential, decoding meaningful information from EEG remains fundamentally challenging due to the low signal-to-noise ratio, temporal non-stationarity, and the inherent heterogeneity of neural activity across individuals and brain regions [7, 13].

Recent advances in deep learning have significantly improved the modeling capacity of EEG decoders. Convolutional and temporal models, such as CNNs, RNNs, and Transformers—have shown great potential in capturing complex spatiotemporal dependencies in EEG recordings [4, 11, 14, 39, 48]. Moreover, trends like large-scale pretraining and self-supervised learning, which revolutionized natural language and vision domains, are starting to demonstrate encouraging results in neural decoding [22, 44, 45, 47, 50, 54]. Despite this progress, most existing EEG models implicitly assume a homogeneous cortical structure, processing the entire electrode montage as a single unified source. This assumption overlooks the brain’s well-established functional modularity, where distinct cortical regions exhibit specialized dynamics and contribute differently to cognitive processes. As a consequence, global models often overfit to noise-rich whole-brain signals, while region-aware variants underutilize cross-regional complementarities [6, 8, 18, 29, 32]. To address these limitations, recent efforts have explored multi-band modeling, region-specific attention, subject-adaptive learning, and dynamic neural representations [3, 15, 34, 38]. However, these approaches remain fundamentally monolithic—they

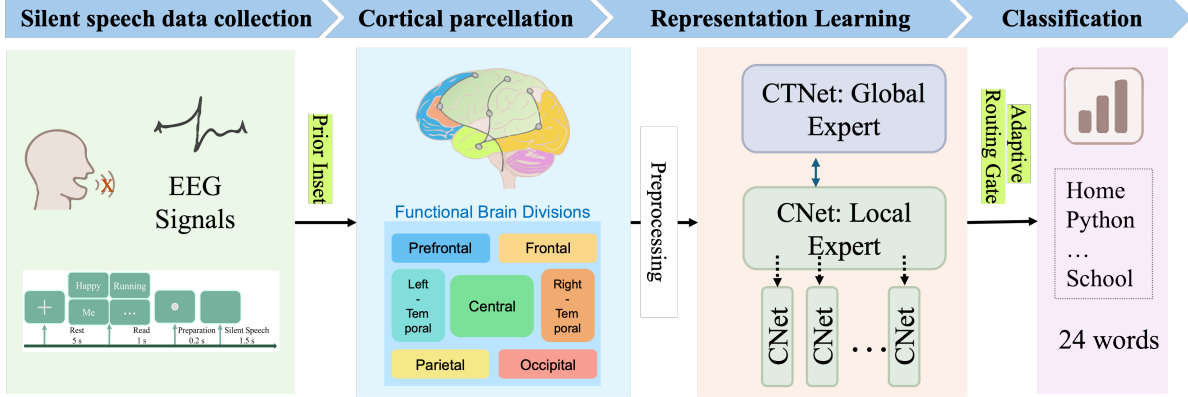


Figure 1. Overall illustration of EEG-based text decoding using BrainStack.

lack an explicit mechanism to model the brain as a collection of interacting functional modules or to coordinate region-specific learners in a principled manner.

The latest methods have adopted channel-wise tokenization strategies—treating each electrode as an independent sequence unit fed into Transformer backbones [11, 28]. While this formulation aligns with attention mechanisms and facilitates efficient temporal modeling, it inherently ignores anatomical clustering and spatial continuity. Consequently, it overlooks the physiologically grounded inter-regional dependencies that shape neural representations [7, 39, 53]. This limitation becomes especially pronounced in silent-speech decoding, where fine-grained, cross-regional activation patterns are essential for distinguishing subtle internal articulatory states [16, 37, 40, 49].

In contrast, neuroscience offers strong motivation to respect the brain’s functional heterogeneity. Neuroscientific research has long emphasized the modular organization of the brain, with distinct cortical areas associated with specific cognitive roles [26], especially language [21, 33, 35]. Classical anatomical studies consistently parcellate the cortex into functional modules—prefrontal, temporal, parietal, and occipital regions—each associated with distinct cognitive pathways [43]. Neural activity during cognitive and linguistic tasks is therefore spatiotemporal and distributed, with region-specific activation patterns reflecting executive control, articulatory planning, auditory–semantic processing, and visual integration [2, 5, 24, 30]. These insights highlight the importance of functionally informed architectures that explicitly respect regional specialization to exploit the diversity of cortical dynamics and enhance generalization [25]. While some recent studies have begun to incorporate region-aware modeling into EEG decoding, many still rely on simplified channel selection schemes or majority-voting ensembles, which are insufficient to capture the rich, cooperative dynamics across regions [1, 9]. Simple decision-level fusion strategies also struggle to generalize in low-data or high-noise regimes, where modeling

the interaction between global and local representations becomes particularly important [51]. Graph-based approaches such as LGGNet have made initial progress toward incorporating region priors, but they generally adopt homogeneous encoders and static connectivity patterns, limiting their ability to capture dynamic coordination between scales [10].

To overcome these limitations, we introduce BrainStack, a functionally guided Neuro–Mixture-of-Experts (Neuro-MoE) framework designed for robust EEG-based language decoding. Motivated by the brain’s modular organization, BrainStack partitions the EEG input into anatomically defined cortical regions and assigns each region to a specialized expert network, while a transformer-based global expert models long-range dependencies and whole-brain contextual interactions. Each regional expert uses a lightweight convolutional encoder to capture localized neural dynamics, whereas the global expert integrates broader temporal–spatial structure through a hybrid convolution–attention design. To coordinate these heterogeneous experts, BrainStack employs an adaptive expert routing gate that assigns context-dependent routing weights to expert representations and aggregates them through a learnable routing mechanism. To further enhance intra-expert coherence, we employ cross-regional hierarchical distillation in which the global expert provides top-down semantic guidance to regional experts. By aligning their output distributions, the distillation encourages each expert to learn not only region-specific cues but also the global semantic structure underlying silent-speech representations.

Our overarching objective is to develop an efficient and generalizable EEG decoder capable of exploiting complementary neural signals across distributed cortical modules. BrainStack achieves this by combining functional modularity, adaptive expert routing, and hierarchical distillation within a unified Neuro-MoE formulation—addressing limitations of prior homogeneous or weakly coupled EEG models and improving accuracy, scalability, and interpretability for practical BCI applications. To summarize, our contribu-

tions are as follows.

- We propose BrainStack, a neuroscientifically grounded Neuro-MoE architecture that integrates global and region-specific experts through anatomically guided modularization and adaptive expert routing.
- We introduce a hierarchical cross-regional distillation mechanism in which the global expert supervises regional experts, promoting top-down semantic alignment and robustness under subject variability.
- We present SilentSpeech-EEG (SS-EEG), a large-scale benchmark containing over 120 hours of EEG data from 12 subjects across 24 silent words—the largest dataset for word-level neural decoding to date.

2. Methodology

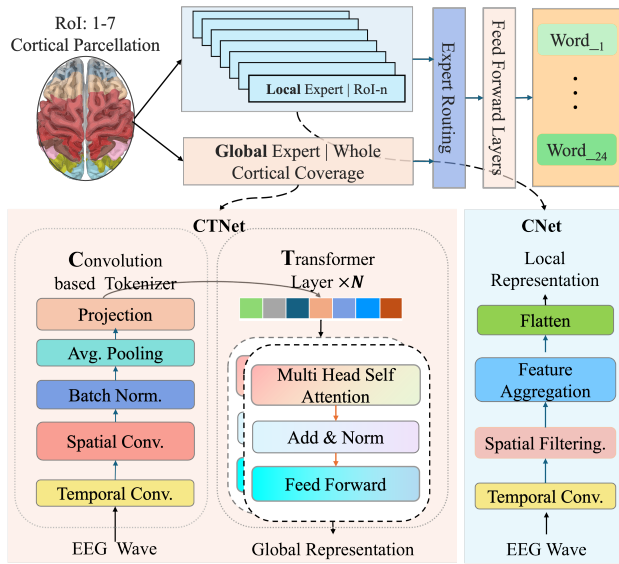


Figure 2. Overview of the proposed BrainStack for EEG-based text decoding. Raw EEG signals $\mathbf{X} \in \mathbb{R}^{C \times T}$ are partitioned into seven region-specific subsets and one global input. Local experts adopt lightweight spatio-temporal CNNs, while the global expert (CTNet) combines CNN and Transformer layers. Outputs are adaptively fused by an expert routing mechanism f_{meta} for final prediction $y \in \mathcal{Y}$.

2.1. Problem Formulation

We formulate EEG-based text decoding as a structured multi-class classification task. Each EEG trial is represented as a matrix $\mathbf{X} \in \mathbb{R}^{C \times T}$, where C denotes the number of channels and T is the number of time steps. The objective is to identify the corresponding cognitive or behavioral class label $y \in \{1, \dots, K\}$. Unlike images or speech, EEG signals are inherently structured by anatomical priors. Channels can be grouped into N functionally defined brain regions, each associated with specific cognitive subfunctions

and distinct signal characteristics. Let \mathbf{X}_i denote the input segment corresponding to region i , and let its task-relevant latent representation $\mathcal{I}_{\text{local}}^i$ be defined as:

$$\mathcal{I}_{\text{local}}^i = \phi_i(\mathbf{X}_i), \quad (1)$$

where $\phi_i(\cdot)$ is a region-specific encoder. Due to anatomical and functional specialization, the regional representations are partially independent in their distribution and semantics.

Cognitive processes depend on coordinated activity across anatomically distinct brain regions, making inter-regional complementarity essential for capturing task-relevant semantics. Because no single region can fully represent complex cognitive states, integrating distributed neural features into a unified representation is necessary. To accommodate task-specific variability—such as the dominance of temporal regions in language decoding or central regions in motor imagery—we model the global neural representation as a weighted aggregation of region-specific features, formally defined as:

$$\mathcal{I}_y = \sum_{i=1}^N \omega_i^y \cdot \mathcal{I}_{\text{local}}^i = \sum_{i=1}^N \omega_i^y \cdot \phi_i(\mathbf{X}_i), \quad (2)$$

where \mathcal{I}_y represents the *task-specific global representation* that integrates region-specific features according to their contextual relevance under task y . The term ω_i^y denotes the learnable importance weight assigned to region i , reflecting its contribution to the task. These weights are dynamically optimized to emphasize anatomically distinct brain regions based on their neural significance.

Finally, the key challenge of EEG decoding lies in balancing regional specialization with cross-region integration, while adapting to task-specific variability. Formally, the decoding objective is to simultaneously learn both the local encoders $\phi_i(\cdot)$ and a fusion function $g(\cdot)$ to yield:

$$\hat{y} = \arg \max_k \left[g \left(\sum_{i=1}^N \omega_i^y \cdot \phi_i(\mathbf{X}_i) \right) \right]_k, \quad (3)$$

where k indexes the set of class labels, and $g(\cdot)$ maps the integrated features into class logits. The arg max operator selects the class with the highest predicted score, resulting in the final output.

2.2. The Proposed Framework: BrainStack

Motivated by the principle that cognition arises from the interplay between distributed global coordination and localized regional computation [51], BrainStack formulates EEG decoding within a Neuro-Mixture-of-Experts paradigm. Specifically, we explicitly decompose each

EEG trial into a global view and seven functionally defined regional views, following canonical anatomical divisions: Prefrontal, Frontal, Central, Left-Temporal, Right-Temporal, Parietal, and Occipital [32]. Formally, each EEG sample $\mathbf{X} \in \mathbb{R}^{C \times T}$ is processed in parallel by a global expert and a set of regional experts, where each expert receives a spatially tailored subset $\mathbf{X}_i \in \mathbb{R}^{C_i \times T}$. This modular decomposition lays the foundation for adaptive expert routing and hierarchical coordination in the subsequent stages of BrainStack.

To ensure each regional expert specialize in extracting discriminative, anatomically grounded features while supporting scalable parallel computation across cortical regions. All experts are trained jointly in an end-to-end manner, facilitating coordinated learning and enabling BrainStack’s Neuro-MoE to effectively integrate both localized and global information [6].

CTNet: Attention-based Global Expert As illustrated in Fig. 2, the global expert is responsible for modeling long-range dependencies and whole-brain contextual interactions. To achieve this, CTNet combines convolutional feature extraction with Transformer-based sequence modeling, enabling it to capture both fine-grained temporal dynamics and cross-regional coordination across the full electrode montage. The input to the global expert is a preprocessed EEG trial $\mathbf{X} \in \mathbb{R}^{C \times T}$, where C denotes the number of channels and T the number of time steps. CTNet processes this input through two primary stages: a convolutional patch embedding module that transforms raw EEG segments into latent tokens, and a Transformer encoder that integrates information across these tokens to form a global, cognitively meaningful representation.

1) Convolutional Patch Embedding. The global expert first converts the continuous EEG waveform into a sequence of latent tokens via a convolutional patch embedding module. A temporal convolution extracts short-duration dynamics within each channel, followed by a spatial convolution that aggregates information across electrodes to capture whole-brain coordination. Batch normalization and ELU activation stabilize training, and average pooling partitions the signal into fixed-length windows, each forming a multi-channel temporal patch. A final 1×1 convolution projects each patch into the latent space, yielding a token sequence $\mathbf{Z} \in \mathbb{R}^{N \times D}$ that is subsequently processed by the Transformer encoder.

2) Transformer Encoder. The resulting patch tokens are processed by a stack of Transformer layers, each composed of multi-head self-attention and feedforward blocks with residual Add–Norm connections. This stage performs global integration across the entire token sequence, enabling the model to capture long-range temporal dependencies and cross-channel interactions that extend beyond the

receptive field of convolutional filters.

Through this process, the global expert produces a set of contextualized representations that summarize whole-brain spatiotemporal dynamics. These global representations are subsequently passed to the expert routing gate, where they are jointly considered with the outputs of the regional experts to determine the final routed prediction.

CNet: Convolution-based Local Expert To complement the global expert, BrainStack incorporates a set of lightweight regional experts, each dedicated to modeling EEG signals from a specific functional cortical area. For each region $n \in 1, \dots, N$ (with $N = 7$), the corresponding input $\mathbf{X}_n \in \mathbb{R}^{C_n \times T}$ is extracted via an anatomically informed channel mapping (standard 10-10/10-20 system), ensuring that $C_n \ll C$ and enabling each expert to focus on localized neural dynamics within its region.

Inspired by the architecture proposed in [27], each regional expert adopts a compact convolutional design tailored for EEG decoding. The module consists of temporal convolutions that capture short-duration temporal structure, depthwise spatial convolutions that learn inter-channel correlations within the region, and separable convolutions that provide efficient feature abstraction. Batch normalization and dropout are applied throughout to ensure stable optimization and mitigate overfitting.

Adaptive Expert Routing Gate To coordinate the global and regional experts, BrainStack employs an adaptive expert routing gate. The router assigns context-dependent routing weights to each expert and aggregates their representations accordingly:

$$F_{\text{meta}} = \sum_{i=1}^N \alpha_i \cdot F_i, \quad (4)$$

where F_i denotes the representation produced by the i -th expert and α_i is the routing coefficient produced by the gate. The coefficients are normalized via a softmax constraint, ensuring $\sum_{i=1}^N \alpha_i = 1$.

Each routing weight α_i is computed through a lightweight scoring function:

$$\alpha_i = \frac{\exp(h(F_i))}{\sum_{j=1}^N \exp(h(F_j))}, \quad (5)$$

where $h(\cdot)$ is a learnable projection that evaluates the relevance of each expert’s representation to the final decision. This mechanism allows the Neuro-MoE to dynamically shift focus among experts, effectively highlighting spatially or temporally informative regions while attenuating noisy or uninformative ones. The routed representation F_{route} is then passed to a final prediction head, implemented as a fully connected layer followed by softmax activation.

Table 1. Comparison of SS-EEG with representative EEG datasets for imagined or silent speech decoding.

Dataset	Subjects	Vocabulary / Classes	Trials	Duration	Channels	Sessions	Repeats per Class
KaraOne [52]	12 (8 usable)	11 (7 phonemes + 4 words)	1056	~4.5 h	64 EEG + 4 EOG	3	12
Thinking Out Loud [36]	10	4 (Spanish words)	2236	~3.5 h	128 EEG + 8 EXG [†]	3	55–60
SS-EEG (Ours)	12 (10 usable)	24 (English words)	60,000	~120 h	128 EEG + 8 EXG [†]	16	250

EXG channels include 4 auxiliary electrodes for eye (EOG) and 2 muscle (EMG) activity monitoring, as well as 2 reference electrodes.

2.3. Hierarchical Multi-Objective Optimization

BrainStack employs a hierarchical multi-objective training strategy that aligns all experts within a unified Neuro-MoE framework. Training is scheduled dynamically, beginning with a global warm-up phase to establish a stable whole-brain representation, and gradually transitioning into full multi-expert supervision encompassing fused prediction, global modeling, regional specialization, and cross-regional distillation [12, 55]. Formally:

$$\mathcal{L}_{\text{total}} = \lambda \cdot \mathcal{L}_{\text{fused}} + \alpha \cdot \mathcal{L}_{\text{global}} + \beta \cdot \mathcal{L}_{\text{local}} + \gamma \cdot \mathcal{L}_{\text{distill}}, \quad (6)$$

where λ , α , β , and γ are hyperparameters controlling the relative weights of each term.

We introduce a dynamic scheduling function to progressively adjust task weights during training. Let $\mathcal{P}(t)$ denote the training progress at epoch t :

$$\mathcal{P}(t) = \min \left(1.0, \frac{\text{epoch} - T_{\text{warmup}}}{T_{\text{transition}}} \right), \quad (7)$$

where T_{warmup} is the duration of the warm-up stage and $T_{\text{transition}}$ controls the duration of the transition phase.

The fused loss weight is then annealed according to:

$$\lambda = (1 - \mathcal{P}(t)) \cdot \lambda_{\min} + \mathcal{P}(t) \cdot \lambda_{\max}, \quad (8)$$

To regulate auxiliary components, we define a shared scheduling function:

$$\omega_{\text{aux}}(x) = x \cdot \mathcal{P}(t) \cdot \left(1 - \min \left(\frac{\mathcal{L}_{\text{fused}}}{\text{max_loss_estimate}}, 1.0 \right) \right) \quad (9)$$

where $\omega_{\text{aux}}(x)$ denotes the dynamic weight of auxiliary supervision and max_loss_estimate is an empirical upper bound on the loss.

The final auxiliary weights are thus:

$$\mathbf{w} = [\omega_{\text{aux}}(\alpha_{\max}), \omega_{\text{aux}}(\beta_{\max}), \omega_{\text{aux}}(\gamma_{\max}) \cdot \mathcal{P}(t)], \quad (10)$$

Hierarchical Distillation Across Experts. To promote coordinated learning within the Neuro-MoE, we adopt a top-down distillation strategy in which the global expert provides semantic guidance to each regional expert. The distillation loss is defined as:

$$\mathcal{L}_{\text{distill}} = \sum_{i=1}^N \text{KL} \left(\text{Softmax} \left(\frac{\mathbf{F}_{\text{global}}}{T} \right) \parallel \text{Softmax} \left(\frac{\mathbf{F}_i}{T} \right) \right) \quad (11)$$

where $\mathbf{F}_{\text{global}}$ and \mathbf{F}_i are the logits from the global and i -th regional expert, respectively, and T is a temperature parameter. This hierarchical objective transfers high-level semantic structure from the global expert to each regional expert, improving their capacity to model fine-grained local patterns while preserving coherence with the fused routed prediction.

3. Experiments

3.1. Dataset

Silent Speech EEG (SS-EEG) To evaluate the proposed Neuro-MoE framework, we introduce SS-EEG, a large-scale dataset tailored for word-level silent speech decoding from EEG signals. SS-EEG contains over 120 hours of recordings from 12 participants, each performing covert articulation of 24 commonly used English words (e.g., “go”, “happy”, “python”) across 16 sessions. With approximately 6,000 trials per subject, the dataset offers dense temporal coverage and robust within- and cross-subject evaluation settings. To the best of our knowledge, SS-EEG is the largest publicly available corpus for word-level silent speech decoding using EEG, and will be released upon publication.

A single session contains 375 silent speech trials and lasts approximately 40 minutes including scheduled breaks. The experimental paradigm follows a four-stage protocol: *rest*, *read*, *preparation*, and *silent speech*. Each trial begins with a 5-second rest phase, including a 1.5-second fixation cross. The target word is then displayed for 1 second during the read phase. A brief 0.2-second auditory cue signals transition into the imagination phase, where the subject silently repeats the word for 1.5 seconds. To minimize fatigue, participants are provided with a break after every 20 trials for up to 5 minutes. EEG signals were recorded using a 128-channel Neuroscan system at a 1000 Hz sampling rate. Signals were band-pass filtered to 1–45 Hz and segmented into clean trial epochs. We further applied per-channel z-score

Table 2. Performance comparison on the SS-EEG dataset for word-level classification.

Model	Param.	S01	S02	S03	S04	S05	S06	S07	S08	S09	S10	Avg. Acc
EEGNet	8.54K	40.80%	35.30%	33.50%	22.90%	17.70%	10.60%	49.60%	14.00%	38.70%	24.70%	28.78%
TCNet	78.62K	36.90%	36.40%	32.70%	22.70%	14.30%	15.30%	44.40%	16.40%	50.40%	25.50%	29.50%
EEGConformer	0.75M	58.20%	32.70%	27.50%	12.20%	11.20%	7.00%	30.90%	7.00%	23.90%	28.30%	23.89%
STTransformer	2.78M	60.30%	16.40%	30.90%	21.30%	17.40%	35.10%	15.60%	31.20%	31.20%	23.40%	28.28%
LaBraM	5.80M	63.40%	13.00%	15.10%	9.10%	8.60%	7.50%	34.30%	8.30%	13.20%	10.40%	18.29%
BrainStack_Homo	5.93M	81.04%	27.79%	32.98%	23.37%	6.23%	11.69%	53.77%	11.69%	60.77%	18.44%	32.78%
BrainStack_RoI5	1.05M	80.26%	39.22%	44.15%	24.94%	5.71%	11.42%	56.10%	15.84%	62.85%	31.42%	37.19%
BrainStack	1.06M	88.05%	39.48%	48.57%	29.87%	10.13%	17.40%	60.25%	19.74%	70.64%	34.54%	41.87%

normalization and removed trials with excessive noise or artifacts. It is noted that due to severe signal contamination in two subjects, the final released dataset includes recordings from 10 participants. For a comprehensive description of the data acquisition protocol and preprocessing pipeline, we refer readers to Section “The SS-EEG Dataset” in the supplementary material.

Thinking out Loud Beyond the primary within-subject evaluation on SS-EEG, we also conduct experiments under a cross-subject protocol as well as on the public Thinking Out Loud dataset [36]. These results, reported in the Appendix under Additional Experiments: Cross-Subject and Public Dataset, further validate the robustness and generalization capacity of the proposed Neuro-MoE framework.

3.2. Evaluation Metric

Evaluation metric. We adopt a session-wise evaluation protocol to avoid data leakage. For each subject, the 16 EEG sessions are split into 14 for training, 1 for validation, and 1 for testing, , ensuring that all splits originate from non-overlapping temporal blocks. Model performance is reported as the average classification accuracy across subjects, following the same evaluation protocol for all baselines.

Baselines. We benchmark BrainStack against a representative suite of state-of-the-art EEG decoding models. The comparison includes two fully supervised CNN-based architectures—EEGNet [27] and TCNet [20]—two Transformer-based models—EEGConformer [42] and STTransformer [41]—and the pre-trained foundation model LaBraM [23].

Implementation Details. The model is implemented in PyTorch and trained on one NVIDIA A40 GPU using mixed precision. We use stochastic gradient descent (SGD) optimizer with a learning rate of 5×10^{-3} , momentum of 0.9 and weight decay of 1×10^{-4} . The training objective is

defined as a dynamic multi-objective loss (6), combining cross-entropy for classification and KL divergence for distillation with a temperature of 4.0 [17, 46]. Following a 5-epoch warm-up, the fusion loss weight increases linearly from 0.2 to 1.0, while the global supervision weight decays from 0.8 to 0. Regional and distillation weights are further modulated by training progress and the current fused loss. Training proceeds for up to 100 epochs, controlled by early stopping with the patience of 5 epochs.

3.3. Performance Comparison

Table 2 summarizes the classification performance of BrainStack and a diverse set of baseline models on the SS-EEG dataset. Among the baselines, EEGNet and TCNet represent compact CNN-based architectures, while EEGConformer and STTransformer are attention-based designs. LaBraM serves as a large-scale pretrained foundation model.

BrainStack achieves the best overall performance with an average accuracy of 41.87%, outperforming all baselines and model variants. Compared to the strongest baseline (TCNet, 29.50%), BrainStack delivers a significant improvement of +12.37%. Notably, it achieves the highest accuracy on 8 out of 10 subjects, and remains highly competitive on the remaining ones, reflecting strong generalization across individuals.

Comparisons with model variants further highlight the benefits of the proposed Neuro-MoE formulation. BrainStack_ROI5 (37.19%), which adopts a coarser 5-region anatomical partition, lags behind by 4.68%, underscoring the importance of fine-grained, functionally guided cortical decomposition. Likewise, BrainStack_Homo (32.78%), which replaces heterogeneous experts with identical CTNet encoders across all branches, performs significantly worse despite having more than five times the parameter count. Finally, BrainStack surpasses LaBraM (18.29%) by a wide margin while using only one-fifth of the parameters (1.06M vs. 5.80M), emphasizing that task-specific architectural design and hierarchical expert coordination are more effective than model size alone for low-SNR neural decoding tasks.

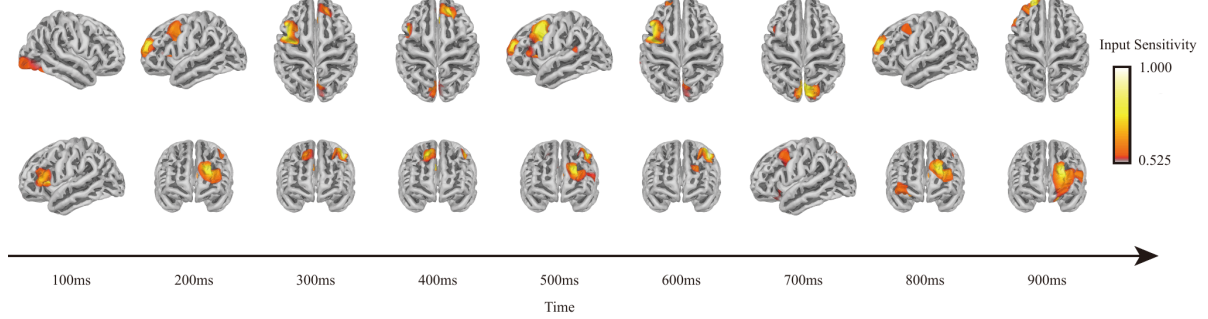


Figure 3. Human attention dynamics during silent speech execution. Temporal evolution of brain activation maps obtained through attribution analysis. The maps illustrate the spatiotemporal distribution of sensitivity in response to the input stimulus across different brain regions from 100ms to 900ms. Warmer colors represent higher sensitivity, indicating stronger contribution to the model’s decision at each time step. Each vertical pair of cortical maps represents two complementary views of the brain at the same moment, offering a clearer visualization of region-specific activations. The analysis captures the progression of localized neural responses transitioning into broader inter-regional integration, revealing both independent regional dynamics and global coordination underlying silent speech decoding.

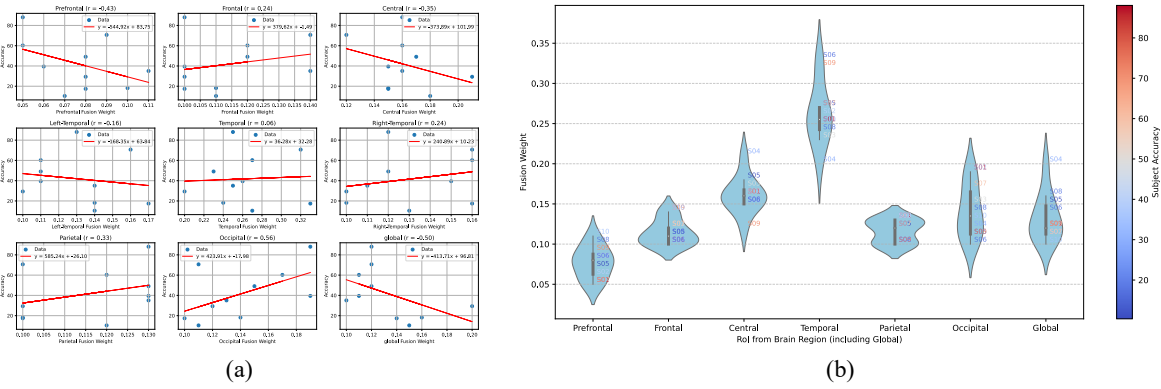


Figure 4. Regional contribution analysis in the adaptive routing gate. (a) Correlation between average fusion weight of each region and subject-level accuracy, with fitted regression lines and Pearson’s r . (b) Violin plots of weight distributions across experts, overlaid with subject accuracies (color-coded), highlighting variability in regional importance.

To assess subject-specific consistency, we report accuracy and F1-score for each of the 10 test subjects, averaged over three random seeds. As shown in Figure 5, substantial inter-subject variability is observed. Overall, the error bars illustrate a clear pattern: strong stability in high-performing subjects and pronounced variability in weaker ones. High-performing subjects (e.g., S01, S07, S09) achieve accuracies above 60% with minimal variance, indicating stable and reliable neural patterns. Notably, S01 reaches 88.05% accuracy and 0.88 F1, the highest across all subjects. In contrast, low-performing subjects (e.g., S05, S06, S08) exhibit both low accuracy (S05: 10.13%) and large seed-dependent fluctuations, reflecting sensitivity to noise and inconsistent neural responses. The trend highlights the value of BrainStack’s modular expert design and adaptive routing, which help manage subject-specific neural heterogeneity.

To evaluate the contribution of each cortical region, we analyze the learned expert routing weights. As shown in Fig. 4(a), the Occipital expert exhibits the strongest positive

correlation with subject-level accuracy ($r = 0.56$), highlighting the importance of visual-cortical activity for silent-speech decoding. In contrast, the Global expert shows a moderate negative correlation ($r = -0.50$), suggesting that excessive reliance on holistic features may be suboptimal. Prefrontal and Central experts show mild negative trends, whereas Parietal and Frontal experts are weakly positive. Temporal experts, though weakly correlated ($r = 0.06$), maintain consistently high routing weights across subjects. Fig. 4(b) further shows that high-performing subjects (e.g., S05, S09) assign greater weight to Temporal and Occipital experts, indicating their complementary predictive value. Overall, these patterns demonstrate that the routing gate not only prioritizes highly informative regions but also leverages stable contributors to enhance generalization.

3.4. Ablation Study

To evaluate the contributions of individual components in our framework, we conduct ablation studies on three key

Table 3. Ablation study on expert architecture, routing mechanism, and loss design.

Objective	Model	Param.	S01	S02	S03	S04	S05	S06	S07	S08	S09	S10	Avg. Acc
Expert architecture	Local only-CNet	0.18M	78.44%	28.83%	22.59%	17.14%	6.23%	4.41%	53.77%	12.47%	57.14%	27.53%	30.86%
	Homogeneous-CNet	0.20M	70.65%	34.02%	36.36%	22.86%	4.94%	3.38%	55.06%	12.47%	62.08%	34.29%	33.61%
	Global only-CTNet	1.01M	72.47%	28.05%	44.41%	24.94%	8.31%	10.38%	56.62%	15.32%	65.71%	28.83%	35.50%
Routing Mechanism and Loss Design	Homogeneous-CTNet	5.93M	81.04%	27.79%	32.98%	26.75%	6.23%	11.69%	53.77%	11.69%	60.77%	18.44%	33.12%
	Token-level fusion	5.21M	82.33%	29.61%	32.98%	14.28%	9.09%	11.17%	34.55%	12.73%	42.86%	24.45%	29.41%
	w/o knowledge distillation	1.06M	84.94%	29.87%	38.70%	17.14%	5.97%	14.03%	54.03%	14.55%	70.38%	27.27%	35.69%
	w/o warm-up	1.06M	84.42%	34.54%	29.87%	12.98%	7.01%	12.47%	56.62%	16.6%	55.58%	29.61%	33.97%
Ours	BrainStack	1.06M	88.05%	39.48%	48.57%	29.87%	10.13%	17.40%	60.25%	19.74%	70.64%	34.54%	41.87%

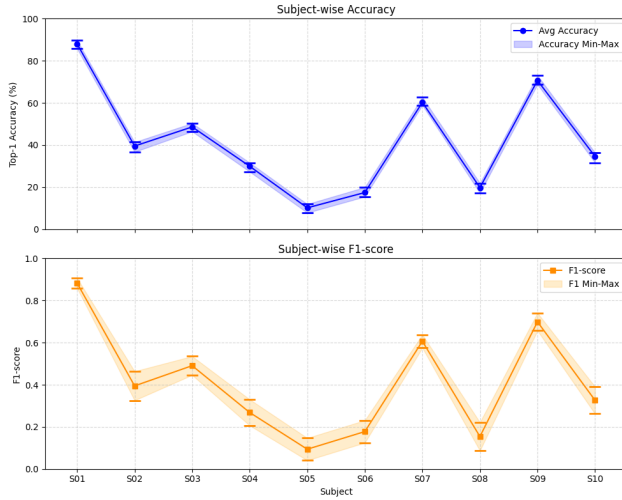


Figure 5. Subject-wise performance variability across three random seeds. Top: classification accuracy with min–max error bands. Bottom: F1-score with corresponding min–max range.

aspects of BrainStack: (1) the expert architecture, (2) the expert routing mechanism, and (3) the hierarchical loss design. Results across ten subjects are reported in Table 3.

Ensemble architecture. We examine four architectural variants to assess the impact of structural design. The *Local only-CNet* configuration aggregates predictions from independent regional CNN experts and achieves 30.86%, confirming the limited capability of purely local modeling without global coordination. Introducing structural consistency through *Homogeneous-CNet* yields a small improvement (33.61%), while *Global only-CTNet* reaches a stronger 35.50%, validating the necessity of whole-brain contextual information. The strongest homogeneous variant, *Homogeneous-CTNet* (33.12%), applies identical CTNet encoders across all experts but still falls short of capturing distributed neural dynamics effectively. In contrast, full BrainStack attains 41.87% by combining heterogeneous global and regional experts and aligning them through anatomically in-

formed functional decomposition. These results demonstrate that structural diversity, expert specialization, and functionally guided modularization are more effective than either global or local modeling alone.

Expert routing mechanism and hierarchical loss design.

To assess the role of routing and training objectives, we evaluate token-level fusion and partial loss configurations. The token-level fusion baseline employs an attention-based aggregator over intermediate tokens but performs poorly (29.4%), indicating that shallow token integration is insufficient without heterogeneous experts and richer contextual modeling.

Ablations on the loss design show that removing global-to-local distillation reduces performance to 35.69%, while omitting the warm-up schedule further drops accuracy to 33.97%. These results highlight that adaptive expert routing, hierarchical distillation, and progressive optimization are essential for stable training and effective coordination within the Neuro-MoE.

4. Conclusion

We present BrainStack, the first functionally guided Neuro–Mixture-of-Experts framework for EEG-based neural language decoding. BrainStack unifies global and region-specific neural representations through heterogeneous experts and an adaptive expert routing gate, enabling anatomically grounded and context-aware integration of distributed cortical signals. To support coordinated expert learning, we introduce a hierarchical multi-objective training strategy with progressive scheduling, effectively combining global supervision, regional specialization, and cross-regional distillation. We further release SilentSpeech-EEG (SS-EEG), a large-scale benchmark containing over 120 hours of recordings, making it the most extensive dataset available for word-level silent speech decoding. Comprehensive evaluations—including within-subject, cross-subject, and additional tests on the Thinking Out Loud dataset—demonstrate that BrainStack achieves state-of-the-art performance and strong generalization.

References

[1] N. I. Abbasi, S. Saint-Auret, J. Hamano, A. Chaudhury, A. Bezerianos, N. Thakor, and A. Dragomir. Eeg functional modularity analysis reveals differences in perception of positively-valenced stimuli. In *Springer Lecture Notes in Computer Science*, 2020. 2

[2] G. K. Anumanchipalli, J. Chartier, and E. F. Chang. Speech synthesis from neural decoding of spoken sentences. *Nature*, 568(7753):493–498, 2019. 2

[3] S. Bian, P. Kang, J. Moosmann, M. Liu, P. Bonazzi, R. Rosipal, and M. Magno. On-device learning of eegnet-based network for wearable motor imagery brain-computer interface. In *Proceedings of ACM/IEEE Embedded Systems Week*, 2024. 1

[4] B. Cao, H. Niu, J. Hao, and G. Wang. Building eeg-based cad object selection intention discrimination model using convolutional neural network (cnn). *Advanced Engineering Informatics*, 52:101548, 2022. 1

[5] L. Cao, D. Huang, Y. Zhang, X. Jiang, and Y. Chen. Brain decoding using fnirs. In *Proceedings of the AAAI Conference on Artificial Intelligence*, pages 12602–12611, 2021. 2

[6] X. Chen, T. Jia, and D. Wu. Accurate, robust and privacy-preserving brain-computer interface decoding. *arXiv preprint arXiv:2412.11390*, 2024. 1, 4

[7] B. J. Choi. Geometric machine learning on eeg signals. In *ICASSP*, 2025. 1, 2

[8] Z. Deng, C. Li, R. Song, X. Liu, R. Qian, and X. Chen. Eeg-based seizure prediction via hybrid vision transformer and data uncertainty learning. *Engineering Applications of Artificial Intelligence*, 123:106401, 2023. 1

[9] K. Ding, Y. Chen, R. Bose, L. E. Osborn, A. Dragomir, and N. V. Thakor. Sensory stimulation modulates adaptability of cortical large-scale systems. *Scientific Reports*, 12, 2022. 2

[10] Yi Ding, Neethu Robinson, Chengxuan Tong, Qiuhan Zeng, and Cuntai Guan. Lggnnet: Learning from local-global-graph representations for brain–computer interface. *IEEE Transactions on Neural Networks and Learning Systems*, 35(7):9773–9786, 2023. 2

[11] Y. Ding, J. H. Lee, S. Zhang, T. Luo, and C. Guan. Decoding human attentive states from spatial-temporal eeg patches using transformers. In *Proceedings of the AAAI Conference on Artificial Intelligence*, 2025. 1, 2

[12] S. Du, S. You, X. Li, J. Wu, F. Wang, C. Qian, and C. Zhang. Agree to disagree: Adaptive ensemble knowledge distillation in gradient space, 2020. 5

[13] T. Duan, Z. Wang, G. Doretto, F. Li, C. Tao, and D. Adjeroh. Replay with stochastic neural transformation for online continual eeg classification. In *Proceedings of the IEEE International Conference on Bioinformatics and Biomedicine (BIBM)*, pages 1874–1879, 2023. 1

[14] T. Duan, Z. Wang, G. Doretto, F. Li, C. Tao, and D. Adjeroh. Replay with stochastic neural transformation for online continual eeg classification. In *IEEE International Conference on Bioinformatics and Biomedicine (BIBM)*, pages 1874–1879, 2023. 1

[15] A. Duggento, M. De Lorenzo, S. Bargione, A. Conti, V. Catrambone, G. Valenza, and N. Toschi. An intertwined neural network model for eeg classification in brain-computer interfaces. *arXiv preprint arXiv:2208.08860*, 2022. 1

[16] N. Fitriah, H. Zakaria, and T. L. E. Rajab. Eeg-based silent speech interface and its challenges: A survey. *International Journal of Advanced Computer Science and Applications*, 2022. 2

[17] Shayan Mohajer Hamidi, Xizhen Deng, Renhao Tan, Linfeng Ye, and Ahmed Hussein Salamah. How to train the teacher model for effective knowledge distillation. In *European Conference on Computer Vision*, pages 1–18. Springer, 2024. 6

[18] X. Hao and B. Sun. Speed imagery eeg classification with spatial-temporal feature attention deep neural networks. In *IEEE ISCAS*, pages 3438–3442, 2022. 1

[19] B. He. Brain-computer interface: Challenges and opportunities. *Transactions of Japanese Society for Medical and Biological Engineering*, 51(Supplement):M–148, 2013. 1

[20] Thorir Mar Ingolfsson, Michael Hersche, Xiaying Wang, Nobuaki Kobayashi, Lukas Cavigelli, and Luca Benini. Eegtcnet: An accurate temporal convolutional network for embedded motor-imagery brain–machine interfaces. In *2020 IEEE International Conference on Systems, Man, and Cybernetics (SMC)*, pages 2958–2965. IEEE, 2020. 6

[21] M. Jamali, B. Grannan, J. Cai, A. R. Khanna, W. Muñoz, I. Caprara, A. C. Paulk, S. S. Cash, E. Fedorenko, and Z. M. Williams. Semantic encoding during language comprehension at single-cell resolution. *Nature*, 631(8021):610–616, 2024. 2

[22] Wei-Bang Jiang, Yansen Wang, Bao-Liang Lu, and Dongsheng Li. Neurolm: A universal multi-task foundation model for bridging the gap between language and eeg signals. *arXiv preprint arXiv:2409.00101*, 2024. 1

[23] Wei-Bang Jiang, Li-Ming Zhao, and Bao-Liang Lu. Large brain model for learning generic representations with tremendous eeg data in bci. *arXiv preprint arXiv:2405.18765*, 2024. 6

[24] X. Jiang, C. Zhou, Y. Duan, Z. Zhao, T. Do, and C.-T. Lin. Neural spelling: A spell-based bci system for language neural decoding. *arXiv preprint arXiv:2501.17489*, 2025. 2

[25] W. Johnston and S. Fusi. Modular representations emerge in neural networks trained to perform context-dependent tasks. *bioRxiv*, 2024. 2

[26] K. Lashley. Theories of brain organization focus on two distinct, but complementary principles: modularity and network connectivity, 2006. 2

[27] Vernon J Lawhern, Amelia J Solon, Nicholas R Waytowich, Stephen M Gordon, Chou P Hung, and Brent J Lance. Eegnet: A compact convolutional neural network for eeg-based brain–computer interfaces. *Journal of neural engineering*, 15(5):056013, 2018. 4, 6

[28] Y. E. Lee and S. H. Lee. Eeg-transformer: Self-attention from transformer architecture for decoding eeg of imagined speech. In *2022 10th International Winter Conference on Brain-Computer Interface (BCI)*, pages 1–4, 2021. 2

[29] H. Li and Y. Fan. Unsupervised deep learning for individualized brain functional network identification. *arXiv preprint arXiv:2012.06494*, 2020. 1

[30] S. Li, Y. Chen, P. Ren, Z. Li, J. Zhang, and X. Liang. Highly connected and highly variable: A core brain network during resting state supports propofol-induced unconsciousness. *Human Brain Mapping*, 44(3):841–853, 2022. 2

[31] Z. Liang, Z. Zheng, W. Chen, Z. Pei, J. Wang, and J. Chen. A novel deep transfer learning framework integrating general and domain-specific features for eeg-based brain-computer interface. *Biomedical Signal Processing and Control*, 95: 106311, 2024. 1

[32] Z. Liang, Z. Zheng, W. Chen, Z. Pei, J. Wang, and J. Chen. A novel deep transfer learning framework integrating general and domain-specific features for eeg-based brain-computer interface. *Biomedical Signal Processing and Control*, 95: 106311, 2024. 1, 4

[33] Y. Liu, Z. Zhao, M. Xu, H. Yu, Y. Zhu, J. Zhang, L. Bu, X. Zhang, J. Lu, Y. Li, D. Ming, and J. Wu. Decoding and synthesizing tonal language speech from brain activity. *Science Advances*, 9(23):eadeh0478, 2023. 2

[34] X. Lou, X. Li, H. Meng, J. Hu, M. Xu, Y. Zhao, J. Yang, and Z. Li. Eeg-dbnet: A dual-branch network for temporal-spectral decoding in motor-imagery brain-computer interfaces. arXiv preprint arXiv:2405.16090, 2024. 1

[35] S. Luo, M. Angrick, C. Coogan, D. N. Candrea, K. Wyse-Sookoo, S. Shah, Q. Rabbani, G. W. Milsap, A. R. Weiss, W. S. Anderson, et al. Stable decoding from a speech bci enables control for an individual with als without recalibration for 3 months. *Advanced Science*, 10(35):2304853, 2023. 2

[36] Nicolás Nieto, Victoria Peterson, Hugo Leonardo Rufiner, Juan Esteban Kamienkowski, and Ruben Spies. Thinking out loud, an open-access eeg-based bci dataset for inner speech recognition. *Scientific data*, 9(1):52, 2022. 5, 6

[37] M. Rekrut, M. Sharma, M. Schmitt, J. Alexandersson, and A. Krüger. Decoding semantic categories from eeg activity in silent speech imagination tasks. In *2021 9th International Winter Conference on Brain-Computer Interface (BCI)*, pages 1–7, 2021. 2

[38] O. Shevchenko, S. Yeremeieva, and B. Laschowski. Comparative analysis of neural decoding algorithms for brain-machine interfaces. bioRxiv, 2024. 1

[39] E. Shi, S. Yu, Y. Kang, J. Wu, L. Zhao, D. Zhu, J. Lv, T. Liu, X. Hu, and S. Zhang. Meet: A multi-band eeg transformer for brain states decoding. *IEEE Transactions on Biomedical Engineering*, 2023. 1, 2

[40] R. Song, X. Zhang, X. Chen, X. Chen, X. Chen, S. Yang, and E. Yin. Decoding silent speech from high-density surface electromyographic data using transformer. *Biomedical Signal Processing and Control*, 80:104298, 2023. 2

[41] Yonghao Song, Xueyu Jia, Lie Yang, and Longhan Xie. Transformer-based spatial-temporal feature learning for eeg decoding. arXiv preprint arXiv:2106.11170, 2021. 6

[42] Yonghao Song, Qingqing Zheng, Bingchuan Liu, and Xiaorong Gao. Eeg conformer: Convolutional transformer for eeg decoding and visualization. *IEEE Transactions on Neural Systems and Rehabilitation Engineering*, 31:710–719, 2022. 6

[43] K. E. Stephan, L. Harrison, S. J. Kiebel, O. David, W. Penny, and K. Friston. Dynamic causal models of neural system dynamics, 2006. 2

[44] M. Svanera, A. Morgan, L. S. Petro, and L. Muckli. A self-supervised deep neural network for image completion resembles early visual cortex fmri activity patterns for occluded scenes. *Journal of Vision*, 21(7):5, 2021. 1

[45] Y. Tang, W. Huang, R. Liu, and Y. Yu. Learning interpretable brain functional connectivity via self-supervised triplet network with depth-wise attention. *IEEE Journal of Biomedical and Health Informatics*, 2024. 1

[46] Z. Tu, X. Liu, and X. Xiao. A general dynamic knowledge distillation method for visual analytics. *IEEE Transactions on Image Processing*, 31:6517–6531, 2022. 6

[47] Guangyu Wang, Wenchao Liu, Yuhong He, Cong Xu, Lin Ma, and Haifeng Li. Eegpt: Pretrained transformer for universal and reliable representation of eeg signals. *Advances in Neural Information Processing Systems*, 37:39249–39280, 2024. 1

[48] Jiquan Wang, Sha Zhao, Zhiling Luo, Yangxuan Zhou, Haiteng Jiang, Shijian Li, Tao Li, and Gang Pan. Cbramod: A criss-cross brain foundation model for eeg decoding. *arXiv preprint arXiv:2412.07236*, 2024. 1

[49] Y. Wang, M. Zhang, R. Wu, H. Gao, M. Yang, Z. Luo, and G. Li. Silent speech decoding using spectrogram features based on neuromuscular activities. *Brain Sciences*, 10(7): 442, 2020. 2

[50] W. Wu, W. Wang, K. Jiang, X. Xu, and R. Hu. Self-supervised learning on a lightweight low-light image enhancement model with curve refinement. In *IEEE ICASSP*, pages 1890–1894, 2022. 1

[51] Q. Yue, R. Martin, S. Fischer-Baum, A. I. Ramos-Nuñez, F. Ye, and M. W. Deem. Brain modularity mediates the relation between task complexity and performance. *bioRxiv*, 2017. 2, 3

[52] Shunan Zhao and Frank Rudzicz. Classifying phonological categories in imagined and articulated speech. In *2015 IEEE international conference on acoustics, speech and signal processing (ICASSP)*, pages 992–996. IEEE, 2015. 5

[53] H. Zheng, H. Wang, W. Jiang, Z. Chen, L. He, P. Lin, P. Wei, G. Zhao, and Y. Liu. Du-in: Discrete units-guided mask modeling for decoding speech from intracranial neural signals. *Advances in Neural Information Processing Systems*, 37:79996–80033, 2024. 2

[54] Q. Zhu, X. Zhao, J. Zhang, Y. Gu, C. Weng, and Y. Hu. Eeg2vec: Self-supervised electroencephalographic representation learning. In *IEEE ICASSP*, 2023. 1

[55] G. Zoumpourlis and I. Patras. Motor imagery decoding using ensemble curriculum learning and collaborative training, 2024. 5